A TRANSONIC DOUBLET LATTICE METHOD FOR GENERAL CONFIGURATIONS

L H van Zyl
Aerotek, CSIR
Pretoria, South Africa

Abstract

In this paper a method is developed for applying the Transonic Doublet Lattice Method (TDLM) of Lu and Voβ to general configurations consisting of multiple non-coplanar lifting surfaces and bodies. In the TDLM, the flow around harmonically oscillating surfaces is described by superposition of a steady transonic mean flow and an unsteady harmonic flow. The unsteady flow component is modelled by acceleration potential doublets on the mean wing surface and a source distribution in the flow field near the wing. The time-linearized unsteady transonic small perturbation equation is solved by an integral equation method. A simple implementation of this method for general configurations would result in a prohibitive number of unknown singularity strengths to solve. By dividing the lifting surfaces of the configuration into groups and limiting the influence of the volume elements to their own group, a sufficiently accurate solution for aeroelastic analyses can be obtained with reasonable memory requirements and computational effort. A simple rectangular wing is used for numerical experiments with the method, and the wing together with a body is used to demonstrate its applicability to wing-body combinations.

Introduction

The calculation of unsteady air loads acting on an aircraft vibrating in its natural modes is a fundamental step in any aeroelastic analysis. The DLM[1,2,3] is used extensively for unsteady subsonic load calculation. Similar methods for supersonic flow[4,5] have also been developed and are being used routinely. Transonic unsteady aerodynamics poses a special challenge because the approximations which are used in subsonic and supersonic flow calculations are not justifiable in transonic flow. Lu and Voβ proposed the TDLM[6] as a solution to the unsteady transonic problem. The TDLM uses volume elements over lifting surfaces in regions where the mean flow is transonic, in addition to the lifting surface elements of the DLM to model the unsteady flow. Each volume element contains a source distribution of unknown strength which is solved along with the doublet strengths of the lifting surface elements. Typically eight layers of volume elements are used in the TDLM, and typical DLM models already contain a large number of lifting surface elements. This means that the computer time and memory requirements for solving a typical aeroelastic problem would be prohibitive if it were implemented by simply adding volume elements to each lifting surface. By assuming that the influence of a volume element is limited to a user-defined group of lifting surfaces, these requirements can be reduced to reasonable levels while still producing accurate results.

Nomenclature

A,B,C,D	matrices of influence coefficients
$\tilde{A},\tilde{B},\tilde{D}$	transformed matrices of influence coefficients
c_p	$\frac{p-p_\infty}{\rho_\infty U_\infty^2/2}$ pressure coefficient
G	$\frac{e^{-i\lambda r}}{4\pi r}$ Green's Function
I	identity matrix
k	$\frac{\omega \ell}{U_\infty}$ reduced frequency
K	$(\gamma+1)M_\infty^2/\beta^2$ or Kernel of Integral Equation
ℓ	reference length, usually half of the average wing chord
M_∞	free stream Mach number
p	local pressure
p_∞	free stream pressure
r	$\sqrt{(\xi-x)^2+(\eta-y)^2+(\varsigma-z)^2}$ distance between control point and singularity
U_∞	free stream velocity
w	downwash at lifting surface control point
x,y,z	scaled cartesian coordinates, x by ℓ, y and z by ℓ/β
β	$\sqrt{1-M_\infty^2}$
γ	ratio of specific heats
Δc_p	unsteady pressure coefficient jump across a lifting surface
ΔS, ΔV	Surface, Volume elements
ε	kM_∞^2/β^2
λ	kM_∞/β^2
Φ	velocity potential, scaled by $U_\infty \ell$
φ	transformed velocity potential
ρ_∞	free stream density
σ	volume source distribution

Copyright © 1996 by the AIAA and ICAS. All rights reserved.

Theory

Without discussing the derivation of the TDLM, the starting point for the present work is repeated below.

In the TDLM, lifting surfaces are discretised into trapezoidal panels and the space around the lifting surfaces are discretised into volume elements. Both volume elements and lifting surface elements have unknown singularity strengths associated with them. The singularity strengths are solved from a system of complex linear equations:

$$\begin{aligned} w &= A\Delta c_p + B\sigma \\ \varphi &= C\Delta c_p + D\sigma \end{aligned} \tag{1}$$

where

$$\begin{aligned} A &= \frac{1}{8\pi}\iint_{\Delta S} K(\bar{x}_0,\bar{y}_0)\,d\bar{\xi}\,d\bar{\eta} \\ B &= -\beta e^{i\varepsilon x}\iiint_{\Delta V}(G_{\xi\xi} - i\varepsilon G_{\zeta})\,d\xi\,d\eta\,d\zeta \\ C &= \frac{e^{-i\varepsilon x}}{8\pi\ell}\iint_{\Delta S}\overline{K}(\bar{x}_0,\bar{y}_0)\,d\bar{\xi}\,d\bar{\eta} \\ D &= \iiint_{\Delta V}(G_{\xi} - i\varepsilon G)\,d\xi\,d\eta\,d\zeta \end{aligned} \tag{2}$$

These equations have three unknown vectors Δc_p, φ and σ. Using the relation

$$\sigma = K\Phi^0_x(\varphi_x + i\varepsilon\varphi) \tag{3}$$

σ can be approximated by the finite differentiation of φ. For a field point $P(x_i, y_j, z_k)$ it holds that

$$\begin{aligned} \sigma_{ijk} &= (1-\mu_{ijk})K\Phi^0_{x_{ijk}}q_{ijk} \\ &+\mu_{i-1,jk}K\Phi^0_{x_{i-1,jk}}q_{i-1,jk} + \mu_{ijk}q_{ijk} - \mu_{i-1,jk}q_{i-1,jk} \end{aligned} \tag{4}$$

where

$$q = \varphi_x + i\varepsilon\varphi$$

and $\mu_{ijk} = 0$ or 1 for sub- or supersonic mean flow field points, respectively. This relation can be expressed as a linear combination

$$\begin{aligned} \{q\} &= [D_1]\{\varphi\} \\ \{\sigma\} &= [D_2]\{q\} \\ \{\sigma\} &= [D_{21}]\{\varphi\} \end{aligned} \tag{5}$$

where

$$D_{21} = D_2 \times D_1$$

σ depends only on φ within the same streamwise bar of volume elements. The matrices D_{21}, D_2 and D_1 for the complete model would all be large, sparse matrices consisting of small square submatrices on the diagonal. These matrices can be calculated and the transformation performed for each bar in turn. By writing the second order Taylor expansion for the function values at points 2 and 3 around point 1, the following expression for the derivative of the function at point 1 is obtained.

$$\begin{aligned} &\frac{df}{dx_1} \\ &= \frac{\left((x_2-x_1)^2 - (x_3-x_1)^2\right)f_1 + (x_3-x_1)^2 f_2 - (x_2-x_1)^2 f_3}{(x_3-x_1)(x_2-x_1)(x_3-x_2)} \end{aligned} \tag{6}$$

The non-zero elements of the first row of D_1 are correspondingly defined by

$$\begin{aligned} D_{1_{1,1}} &= i\varepsilon + \frac{(x_2-x_1)^2 - (x_3-x_1)^2}{(x_3-x_1)(x_2-x_1)(x_3-x_2)} \\ D_{1_{1,2}} &= \frac{(x_3-x_1)^2}{(x_3-x_1)(x_2-x_1)(x_3-x_2)} \\ D_{1_{1,3}} &= \frac{-(x_2-x_1)^2}{(x_3-x_1)(x_2-x_1)(x_3-x_2)} \end{aligned} \tag{7}$$

Non-zero elements of subsequent rows, excluding the last row, are defined by

$$\begin{aligned} D_{1_{i,i-1}} &= \frac{(x_{i+1}-x_i)^2}{(x_{i+1}-x_i)(x_{i-1}-x_i)(x_{i+1}-x_{i-1})} \\ D_{1_{i,i}} &= i\varepsilon + \frac{(x_{i-1}-x_i)^2 - (x_{i+1}-x_i)^2}{(x_{i+1}-x_i)(x_{i-1}-x_i)(x_{i+1}-x_{i-1})} \\ D_{1_{i,j+1}} &= \frac{-(x_{i-1}-x_i)^2}{(x_{i+1}-x_i)(x_{i-1}-x_i)(x_{i+1}-x_{i-1})} \end{aligned} \tag{8}$$

Non-zero elements of the last row are defined by

$$\begin{aligned} D_{1_{n,n-2}} &= \frac{(x_{n-1}-x_n)^2}{(x_{n-1}-x_n)(x_{n-2}-x_n)(x_{n-1}-x_{n-2})} \\ D_{1_{n,n-1}} &= \frac{-(x_{n-2}-x_n)^2}{(x_{n-1}-x_n)(x_{n-2}-x_n)(x_{n-1}-x_{n-2})} \\ D_{1_{n,n}} &= i\varepsilon + \frac{(x_{n-2}-x_n)^2 - (x_{n-1}-x_n)^2}{(x_{n-1}-x_n)(x_{n-2}-x_n)(x_{n-1}-x_{n-2})} \end{aligned} \tag{9}$$

The elements of D_2 are defined by

$$D_{2i,i-1} = \begin{cases} 0 & \text{if point } i-1, j, k \text{ is subsonic} \\ K\Phi^0_{xi-1,jk} - 1 & \text{if point } i-1, j, k \text{ is supersonic} \end{cases}$$

$$D_{2i,i} = \begin{cases} K\Phi^0_{xijk} & \text{if point } i, j, k \text{ is subsonic} \\ 1 & \text{if point } i, j, k \text{ is supersonic} \end{cases} \quad (10)$$

Note that the flow upstream of the first element in the bar can be assumed to be subsonic, therefore $D_{21,0}$ would be zero anyway. The steady c_p value is used to determine whether the mean flow at a point is subsonic or supersonic by comparing it to the critical c_p value, where

$$c_{p_{crit}} = \frac{\left(\frac{1+\frac{\gamma-1}{2}M_\infty^2}{1+\frac{\gamma-1}{2}}\right)^{\frac{\gamma}{\gamma-1}} - 1}{\frac{1}{2}\gamma M_\infty^2} \quad (11)$$

and also to calculate

$$\Phi_x^0 \approx \sqrt{1 - \frac{2}{(\gamma-1)M_\infty^2}\left(\left[\frac{\gamma M_\infty^2 c_p}{2}+1\right]^{\frac{\gamma-1}{\gamma}} - 1\right)} - 1 \quad (12)$$

Substituting equation (5) into equation (1), we get

$$\begin{aligned} w &= A\Delta c_p + BD_{21}\varphi \\ \varphi &= C\Delta c_p + DD_{21}\varphi \end{aligned} \quad (13)$$

or

$$\begin{bmatrix} A & \tilde{B} \\ C & \tilde{D} \end{bmatrix} \begin{Bmatrix} \Delta c_p \\ \varphi \end{Bmatrix} = \begin{Bmatrix} w \\ 0 \end{Bmatrix} \quad (14)$$

where

$$\begin{aligned} \tilde{B} &= B \times D_{21} \\ \tilde{D} &= D \times D_{21} - I \end{aligned} \quad (15)$$

The A sub-matrix is exactly the DLM matrix for this problem. From the second equation,

$$[C]\{\Delta c_p\} + [\tilde{D}]\{\varphi\} = \{0\} \quad (16)$$

or

$$\{\varphi\} = -[\tilde{D}]^{-1}[C]\{\Delta c_p\} \quad (17)$$

If we substitute this into the first equation, we get

$$[A]\{\Delta c_p\} - [\tilde{B}][\tilde{D}]^{-1}[C]\{\Delta c_p\} = \{w\} \quad (18)$$

or

$$[\tilde{A}]\{\Delta c_p\} = \{w\} \quad (19)$$

where

$$\tilde{A} = A - \tilde{B} \times \tilde{D}^{-1} \times C \quad (20)$$

Thus the effect of the TDLM is to modify the DLM influence matrix. Refinements to the TDLM, e.g. the use of a local reduced frequency or Mach number, and limiting the zone of influence of supersonic panels can be incorporated in the calculation of A.

Implementation

Based on the result above, the approach taken in the present work is to replace the submatrix corresponding to the wing-wing influence coefficients of one group in the DLM with the modified sub-matrix as derived above. The cost of implementing the TDLM is the calculation of the influence coefficient matrices B, C and D, the transformations to get to $\tilde{B}$ and $\tilde{D}$, the inversion of $\tilde{D}$ and the transformation to get $\tilde{A}$.

The TDLM was implemented in a DLM which uses axial singularities to model bodies and the method of images to model wing-body interference. In this method, an image of a lifting surface element which is close to a body is formed within the body. The image minimises the velocity normal to the body surface induced by the element and its image.

The output from the DLM for the purpose of aeroelastic analysis are the generalised forces, which depend on the Mach number, reduced frequency and modeshapes. The basic steps involved in the calculation of generalised forces at one Mach number are:

1. Read general and geometric data and modeshapes.
2. Calculate influence coefficients.
3. Solve singularity strengths.
4. Calculate and write generalised forces.

Steps 2 to 4 are repeated for each reduced frequency.

There are numerous possible ways of implementing the method of images in the DLM. In the present case the following rules were applied:

- The maximum radius of any body is used in the generation of images.

- An image of a lifting surface is formed if any edge (left or right) of the element is within 5 body radii from the axis of the body, and the quarter chord point of both edges fall within the axial limits of the body.
- The image of a lifting surface element within one body does not have an image within another body

Likewise, there are many ways of implementing the TDLM. The assumptions used in the present study are:

- Lifting surfaces are grouped by the user. Groups may or may not have volume elements. The user also controls whether the reflection of a group in the case of a symmetric half model is part of the same group or a separate group.
- There is no mutual influence between body elements and volume elements.
- The mutual influence between lifting surface elements and volume elements, and among volume elements, is limited to elements of the same group.
- Images of lifting surface elements do not influence volume elements.
- Volume elements do not contribute to the pressure distribution on bodies in the calculation of generalised forces.

The basic steps in the solution are modified in a number of ways. The volume of the geometric data increases to accomodate the volume elements. Steady c_p data is read together with the geometric and general data. This data is used in the transformations to test whether the mean flow at a point is subsonic or supersonic, and to calculate the elements of D_2 which depend on Φ_x^0.

The biggest change is in the calculation of the influence coefficient matrix. The overall influence coefficient matrix of the DLM is divided into four regions, with the wing-wing influence coefficients at top left, wing-body influence coefficients bottom left, body-wing influence coefficients top right and body-body influence coefficients bottom right. The matrix is calculated column by column, where a column corresponds to a sending element and a row to a receiving element.

The additional wing-volume, volume-wing and volume-volume influence coefficients of the TDLM are stored in separate, temporary matrices. After the wing-wing, wing-body, wing-volume, volume-wing and volume-volume influence coefficients for a particular group have been calculated, the corresponding region of the overall influence coefficient matrix is modified according to equations (15) and (20). The temporary storage is then available for the next group.

The calculation of the body-wing and body-body regions, the solution of the singularity strengths and the calculation of generalised forces proceed exactly as for the DLM.

Additions to the pre-processor for the DLM include provision for defining wing profiles, volume elements and for grouping elements. The pre-processor determines the coordinates of the centres of the volume elements and produces a list of these coordinates. The steady c_p values at these points are then interpolated from CFD results. In the TDLM, a lifting surface is still treated as a flat surface, whereas in the CFD model, a lifting surface has finite thickness. The pre-processor resolves this discrepancy by adding the profile thickness when calculating the coordinates of the volume element centres for interpolation purposes. The ability to display the volume elements of a single group at a time allows quick visual checking of the grouping of lifting surfaces. Figure 1 shows a typical model of a fighter aircraft, with a coarse panelling scheme for clarity, showing the volume regions of all groups. Each wing is divided into three panels to accomodate the control surfaces and the discontinuity in the leading edge. The three panels of each wing belong to a single group. The two stabilisers belong to separate groups. The three panels of the fin belong to single group.

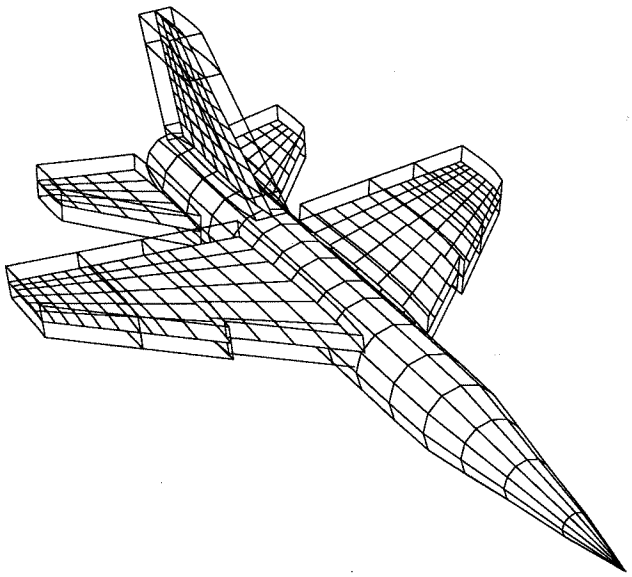

Figure 1. TDLM model of a fighter aircraft.

Results

The test case selected for numerical experiments is a simple wing which will be used for unsteady transonic pressure measurements in a wind tunnel. The wing has an aspect ratio of 4 and a NACA 64A010 profile. At Mach 0.85, the wing shows a large supersonic region, with a shock position that varies from 62% at the root to 55% at 75% span.

Unsteady pressures were solved at two reduced frequencies, zero and 0.1, and for two modes, a pitching mode about the midchord of the wing and a plunging mode. Various panelling schemes were used, viz. an 8

chordwise panels × 6 spanwise strips × 8 layers of volume elements, a 16×6×8 and a 20×12×8 scheme. In the latter scheme, the chordwise divisions were 7*1/16, 8*1/32, 5*1/16. All other divisions were equally spaced. 4 layers of volume elements above and below the wing, extending to 40% of the chord away from the wing reference plane, were used in all cases. Figure 2 shows a symmetric half model of the wing. The calculated steady pressure distributions over the most inboard strip is shown in figure 3 for angles of attack of 0°, 0.5° and 1°. The steady pressures at 0° were used as input to the TDLM, while the pressures at the other angles of attack were used to calculate quasi-steady results for comparison with the TDLM.

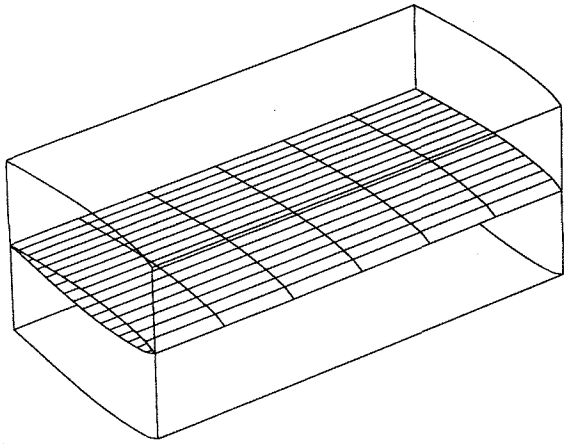

Figure 2. TDLM model of the rectangular wing.

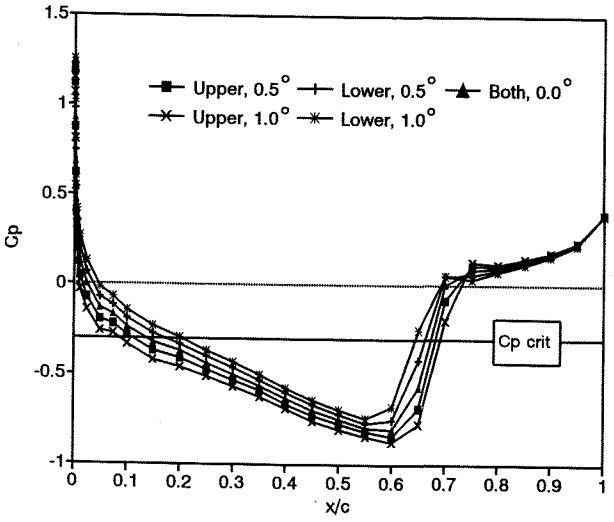

Figure 3. Steady surface pressures over the inboard strip at Mach 0.85 and different angles of attack.

The quasi-steady pressures and unsteady pressures were solved from equation (14) and also from equation (19). Although the results should be identical, the roundoff error may be influenced by the solution method. A DLM solution was also obtained for the 16×6 scheme and the roundoff error determined. Tables 1 and 2 compare the roundoff error of the various panelling schemes and solution methods. In the case of a solution from equation (19), the φ values were obtained from equation (17). The complete solution vector was substituted into the left hand side of equation (14) and a result vector was calculated. The roundoff error is expressed as the rms value of the difference between the new result vector and the original rigth hand side of equation (14). The error values are normalised by the non-dimensional amplitude kh/ℓ in the case of the plunging mode. Separate error values were calculated for the first part, which is the boundary condition and the second part which is related to the transformed velocity potential in the field.

Table 1. Roundoff error, boundary condition ($\times 10^{-6}$)

	Mode 1 k=0	Mode 1 k=0.1	Mode 2 k=0.1
8×6×8, eq (14)	0.650	0.764	0.795
8×6×8, eq (19)	1.623	1.522	1.402
DLM, 16×6	0.759	0.581	0.561
16×6×8, eq (14)	0.827	1.211	1.310
16×6×8, eq (19)	1.865	2.021	1.928
20×12×8, eq (14)	2.867	3.297	2.869
20×12×8, eq (19)	8.896	9.144	8.624

Table 2. Roundoff error, velocity potential ($\times 10^{-6}$).

	Mode k=0	Mode 1 k=0.1	Mode 2 k=0.1
8×6×8, eq (14)	1.386	1.363	1.299
8×6×8, eq (19)	1.161	1.076	0.991
16×6×8, eq (14)	1.990	1.957	1.838
16×6×8, eq (19)	1.653	1.570	1.521
20×12×8, eq (14)	3.556	3.734	3.608
20×12×8, eq (19)	3.918	3.988	3.823

It is clear that the roundoff error is larger when using equation (19) than when using equation (14). This is probably due to the fact that the subdivision of the matrix allows a less efficient pivoting strategy than what is possible with the complete matrix. In absolute terms, however, the roundoff error is acceptably small.

The quasi-steady pressure distribution over the most inboard strip calculated by the TDLM is compared to the quasi-steady results from CFD and the results from the DLM in figure 4. The quasi-steady results from CFD were calculated from both agles of attack to confirm linearity with amplitude. The quasi-steady results show good agreement with results obtained from CFD, while the DLM results expectedly do not show any contribution from the shock motion.

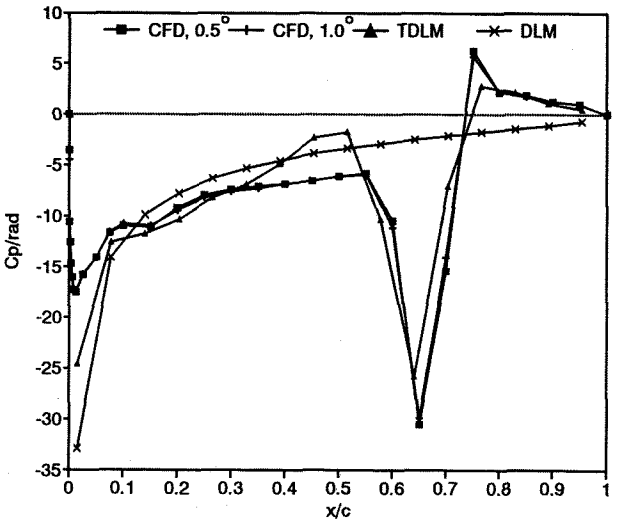

Figure 4. Quasi-steady results for rectangular wing.

Total aerodynamic coefficients were calculated using the different panelling schemes and are compared in tables 3 and 4 for the pitching mode and in table 5 for the plunging mode. The coefficients for the plunging mode were normalised by the non-dimensional amplitude kh/ℓ.

Table 3. Total quasi-steady aerodynamic coefficients for the pitching mode.

	C_L	C_M
8×6×8	5.7705	1.4709
DLM, 16×6	5.2218	1.5155
16×6×8	6.0596	1.3981
20×12×8	5.8374	1.3431

Table 4. Total unsteady aerodynamic coefficients for the pitching mode.

	C_{LR}	C_{LI}	C_{MR}	C_{MI}
8×6×8	5.6080	-0.3161	1.3321	-0.5853
DLM, 16×6	5.0687	-0.1465	1.4180	-0.4603
16×6×8	5.8542	-0.4846	1.2223	-0.6077
20×12×8	5.6536	-0.4503	1.1790	-0.5789

Table 5. Total aerodynamic coefficients for the plunging mode.

	C_{LR}	C_{LI}	C_{MR}	C_{MI}
8×6×8	-0.6471	-5.4922	-0.4970	-1.2984
DLM, 16×6	-0.4250	-4.9902	-0.3923	-1.3925
16×6×8	-0.8396	-5.6866	-0.4916	-1.2006
20×12×8	-0.7886	-5.5005	-0.4691	-1.1573

All figures quoted for the TDLM are from a solution of equation (14). Results from solving equation (19) differs by no more than 1 in the last digit quoted. The differences between the TDLM and DLM results have the same trends as those reported for a similar wing[6].

The wing will not be mounted directly to the wind tunnel wall, but with a fairing as shown in figure 5. This arrangement was used as a test case with a body included. The case was solved with the wing and its reflection in the symmetry plane treated as a single group as well as separate groups. The unsteady pressure distributions over the inboard strip due to symmetric pitching of the wings are shown in figures 6 and 7. The unsteady pressure distributions over the inboard strip due to anti-symmetric pitching of the wings are shown in figures 8 and 9. The lack of significant differences between the results indicates that it is justified in this case to consider the two wings as separate groups.

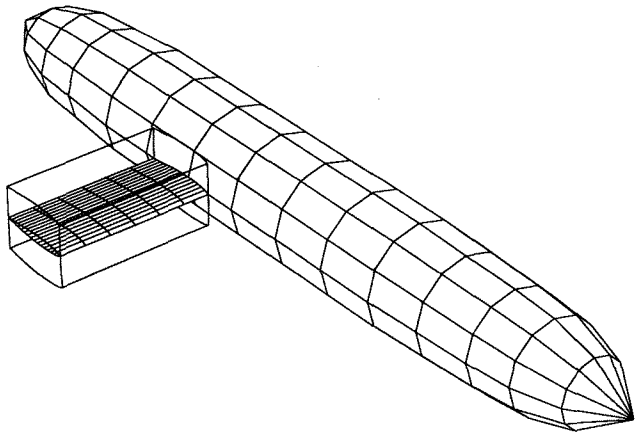

Figure 5. Rectangular wing with fairing.

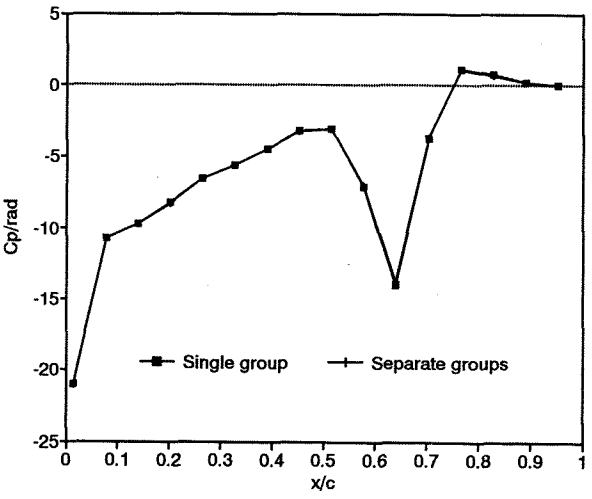

Figure 6. Real part of unsteady pressure due to symmetric pitching.

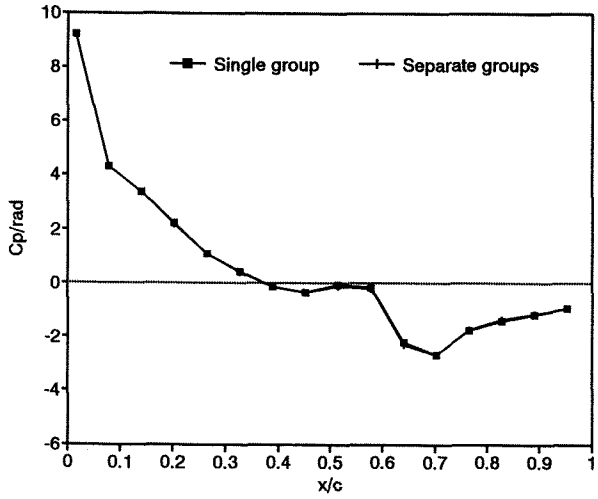

Figure 7. Imaginary part of unsteady pressure due to symmetric pitching.

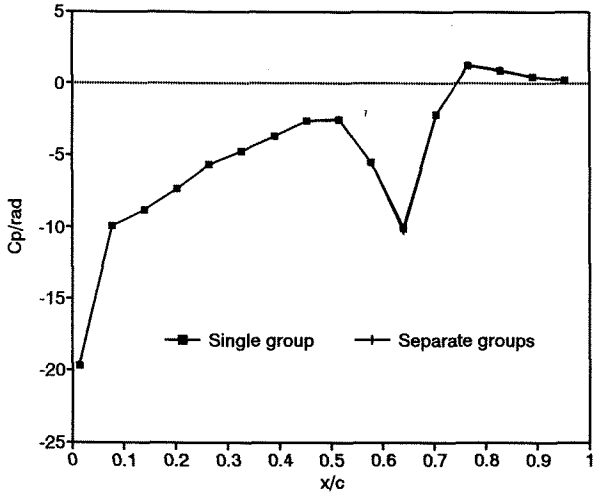

Figure 8. Real part of unsteady pressure due to anti-symmetric pitching.

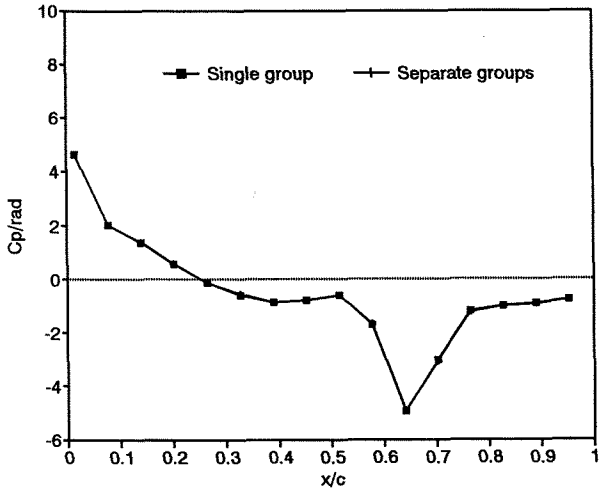

Figure 9. Imaginary part of unsteady pressure due to anti-symmetric pitching.

Conclusion

A method has been developed for implementing the TDLM of Lu and Voβ in a DLM for general configurations. The new method retains the versatility of the DLM and the solid theoretical foundation of the TDLM. The method must still be tested for complex configurations.

References

[1] Kalman, T.P., Rodden, W.P. and Giesing, J.P., "Application of the Doublet-Lattice Method to Nonplanar Configurations in Subsonic Flow", *Journal of Aircraft*, Vol. 8, June 1971, pp. 406-413.

[2] Rodden, W.P. , Giesing, J.P. and Kalman, T.P., "Refinement of the Nonplanar Aspects of the Subsonic Doublet-Lattice Method", *Journal of Aircraft*, Vol. 9, January 1972, pp. 69-73.

[3] Giesing, J.P., Kalman, T.P. and Rodden, W.P., "Subsonic Steady and Oscillatory Aerodynamics for Multiple Interfering Wings and Bodies", *Journal of Aircraft*, Vol. 9, No. 10, October 1972, pp. 693-702.

[4] Chen, P.C. and Liu, D.D., "Unsteady Supersonic Computations of Arbitrary Wing-Body Configurations Including External Stores", *Journal of Aircraft*, Vol. 27, No. 2, February 1990, pp. 108-116.

[5] Van Zyl, L.H., "Modelling of Wing-Body Combinations in Unsteady Supersonic Flow", *Proceedings of the 19th Congress of the International Council of the Aeronautical Sciences*, 1994, Volume 3, pp. 2713-2723.

[6] Lu, S. and Voβ, R., "TDLM - A Transonic Doublet Lattice Method for 3D Potential Unsteady Transonic Flow Calculation", DLR Institut für Aeroelastik, Göttingen, FRG, DLR-FB 92-25, September 1992.